EUKARYOTIC CELL, Oct. 2002, p. 811–822 Vol. 1, No. 5
1535-9778/02/$04.00+0 DOI: 10.1128/EC.1.5.811–822.2002

Maintenance of Mating Cell Integrity Requires the Adhesin Fig2p

Mingliang Zhang, Daniel Bennett, and Scott E. Erdman*

Department of Biology, Syracuse University, Syracuse, New York 13244-1220

Received 11 March 2002/Accepted 22 July 2002

Fungal adhesins represent a large family of serine/threonine-rich secreted glycoproteins. Adhesins have been shown to play roles in heterotypic and homotypic cell-cell adhesion processes, morphogenetic pathways and invasive/pseudohyphal growth, frequently in response to differentiation cues. Here we address the role of the *Saccharomyces cerevisiae* mating-specific adhesin Fig2p. Cells lacking *FIG2* possess a variety of mating defects that relate to processes involving the cell wall, including morphogenetic defects, cell fusion defects, and alterations in agglutination activities. We found that mating-specific morphogenetic defects caused by the absence of *FIG2* are suppressible by increased external osmolarity and that, during mating, *fig2*Δ cells display reduced viability relative to wild-type cells. These defects result from alterations in signaling activated by the mating and cell integrity pathways. Finally, we show that *fig2*Δ zygotes also have defects in zygotic spindle positioning that are osmoremedial, whereas the requirements for *FIG2* in normal cell-cell agglutination and cell fusion during mating are insensitive to changes in the extracellular osmotic environment. We conclude that *FIG2* performs distinct functions in the mating cell wall that are separable with respect to their ability to be suppressed by changes in external osmolarity and that a fundamental role of *FIG2* in mating cells is the maintenance of cell integrity.

Microbial cells regulate their adherence to one another and to components in their environment, including other cell types. In fungi, these interactions take the forms of regulated homotypic adhesion during vegetative growth (flocculation) and regulated heterotypic interactions during mating (agglutination). In symbiotic and pathogenic fungi, additional adhesive interactions occur between fungal cells and cells of plant or animal host tissues. Each of these adhesion interactions enables fungal cells to effectively persist in different environments and to colonize new ones. A general class of proteins, recently recognized for their similarity and termed "adhesins," have been shown to control a number of these cell-cell and cell-environment interactions (18, 20, 46, 58). Adhesins are often relatively large proteins containing an extensive number of residues modified by N-or O-linked glycosylation (25, 38). These proteins are typically maintained on the surface of the cell through a plasma membrane or cell wall-linked glycophosphatidyl inositol (GPI) anchor (38).

An early step of mating in yeast involves the mating factor-induced expression of adhesins that are expressed both commonly and in cell type-specific patterns (27, 56). Induction of agglutinins enables mating cells to modify their adhesion properties so as to specifically adhere to potential mating partners. Loss of any of the agglutinin genes *AGA1*, *AGA2*, or *SAG1*/*AGα 1* from appropriate mating cell types leads to an inability of cells to adhere to mating partners in liquid medium prior to conjugation (reviewed in reference 27). The *FIG2* gene encodes another adhesin-like protein, the expression of which occurs specifically in response to mating pathway activation and in both mating types (15, 47).

Yeast strains deleted for *FIG2* show a suite of phenotypes related to cell surface changes occurring during mating: they display increased agglutination and polarization and show a twofold increase in cell fusion defects relative to the number in wild-type cells (15). Recent studies also indicate that when ectopically expressed, *FIG2* can modify vegetative cell adhesion in liquid culture and during invasive growth (18). *FIG2* encodes a predicted 1,609-amino-acid protein that in its processed form is secreted and becomes cell wall resident due to the presence of a GPI anchor addition site (9, 15). The GPI anchor of Fig2p has been experimentally shown to direct its covalent linkage to the β-1,6 glucan layer of the cell wall (60).

Many of the key features of adhesins relate to their cell wall residency. The fungal cell wall forms a dynamic extracellular matrix that is remodeled in response to growth signals and degraded during cell-cell fusion events. In addition to these morphogenetic roles, the cell wall also serves to localize mannoproteins, including adhesion proteins, which are involved in specialized functions of the cell wall during different phases of the fungal life cycle (25, 38, 55).

Activation of the mating pheromone signaling cascade in *Saccharomyces cerevisiae* leads to cell cycle arrest and repolarization of cell growth in the form of a mating projection, or 'shmoo', toward the source of mating pheromone (the mating partner) (7, 37, 52). A variety of proteins required for cell-cell fusion and subsequent nuclear fusion events are localized to the mating projection tip, permitting the rapid conversion of projections that have made contact into conjugation tubes between the partnered cells (31, 56). The mating-specific adhesins Aga1p, Aga2p, Sag1/Agα 1p, and Fig2p all localize in a polarized manner specifically to the plasma membrane and glucan layers of mating projections, presumably focusing adhesive interactions on this domain of the mating cell specialized for contact-dependent events of mating (15, 18, 27, 56).

The cell wall begins to be remodeled with the onset of projection formation and continues to be remodeled in response to chemotactic and fusogenic signals emanating from mating partners (31, 56). This remodeling in response to po-

* Corresponding author. Mailing address: Department of Biology, Syracuse University, Syracuse, NY 13244-1220. Phone: (315) 443-3748. Fax: (315) 443-2012. E-mail: seerdm@syr.edu.

larized cell growth during mating is both responsive to and partially dependent on signaling through Rho1 and its effector proteins Pkc1 and, most likely, the glucan synthase subunits Fks1 and Gsc2/Fks2 (44, 56). The Rho1/Pkc1 cell integrity pathway functions to closely coordinate cell growth events and the monitoring and maintenance of cell integrity (6, 10, 14, 19, 26). Under conditions of cell wall stress, elements of the Rho1/Pkc1 pathway are essential to the depolarization and subsequent repolarization of the actin cytoskeleton from sites of polarized growth (14, 19). Polarity proteins localized in response to Cdc42p and Rho1p signaling also play important roles in localizing proteins such as Kar9p to sites of microtubule capture at the tips of mating and budding cells (33, 51). These sites are involved in orienting mating cell microtubules during karyogamy and subsequently orienting spindles during mitosis (3, 34, 39). Finally, a role of the Rho1/Pkc1 pathway during mating also appears to occur in the regulation of cell-cell fusion events that are prerequisite for nuclear fusion and zygotic division (42).

Studies of adhesins have revealed their requirements in cell-cell adhesion interactions and morphogenesis; however, little is known concerning the nature of these processes with regard to signaling and whether such functions are related or distinct. Here we report on a novel cell integrity role of the budding yeast adhesin encoded by *FIG2*. We show that a specific subset of the phenotypes shown by cells that lack *FIG2* are osmoremedial under conditions that reduce cell wall stress. We also demonstrate that *fig2*Δ cells display reduced viability in response to mating cell morphogenesis and that the activity levels of the Rho1/Pkc1 pathway are elevated in these cells. Our studies are interesting because they indicate the existence of a feedback relationship in the yeast mating pathway such that a product of a terminal differentiation gene of the pathway, Fig2p, influences signaling in the distinct, but functionally linked, Rho1/Pkc1 cell integrity pathway. This relationship may help to coordinate and ensure proper morphogenesis, cell integrity, and cell fusion during mating under different environmental conditions.

MATERIALS AND METHODS

Yeast growth and manipulation. Yeast growth and sporulation media were as described in reference 54. The strains employed in this study were from either of two derivatives of the S288C background as indicated in Table 1. Bacterial manipulations involving plasmids were performed as described in reference 49. Yeast strains were transformed with plasmids by a modified one-step transformation method (11). Replacements of the *AGA1* gene with *URA3* were made by using a PCR-mediated gene knockout technique (2). *MAT***a** and *MAT*α *aga1*::*URA3 FIG2*::*URA3* double mutants were constructed by mating haploid strains YSE29 and YSE334, selecting for the resulting diploid, sporulating, and selecting tetrad progeny in which *URA3* segregated 2:2. The genotypes for *MAT* and other markers were determined in the candidate double mutant strains, and the presence of disruptions was confirmed by PCR with flanking primers.

Measures of mating cell fusion, morphogenesis, and viability. Analyses of mating yeast cells were carried out as described in reference 15 with the following modifications. Cultures were mixed 1:1 and mated on nitrocellulose filters placed on different media for a period of 4 h. Following mating, cells were either immediately formaldehyde fixed, washed, and stored in 1× phosphate-buffered saline (PBS)–1 M sorbitol at 4°C, or an aliquot of live cells was removed for methylene blue staining to score cell viability, and the remainder of the cells were preserved as described above. Mating projection-conjugation bridge morphogenesis was quantified by analyzing the widths of the parental cells relative to the width of the conjugation bridge joining them in zygotes as described in reference 15. To aid in quantitatively comparing this trait among different strains and under different mating conditions, over 100 zygotes were photographed for each sample with a Nikon TE-300 microscope fitted with a ×100 objective and differential interference contrast (DIC) optics. Images were captured with a Roper/Princeton Instruments MicroMax 5-MHz charge-coupled device (CCD) camera. A ruler tool in Adobe Photoshop was used to determine the three relevant measurements for each zygote. These data were then tablulated and compared by spreadsheet analysis (Excel). A small number of zygotes were discarded from all sample analyses if they met the criterion that the two parental cells differed by more than 0.75× their mean width. These zygotes arise from matings between parental cells of significantly different size; thus, the signaling and growth dynamics of the conjugation bridge joining them are likely to be more variable than those of two similarly sized parents. Typically, removal of these zygotes led to relatively small decreases in the variances of these data. While the morphogenetic effects of *fig2*Δ are most apparent in one of the parental strain backgrounds we have used for the present studies, qualitatively consistent results were found when these experiments were repeated with other S288C-derived *fig2*Δ strains described in this study (Table 1). In this strain background (64), which is more resistant to the cell wall-disturbing effects of calcofluor white relative to the Y800 parental background of YSE21, YSE22, YSE29, and YSE30 (G. Huang and S. Erdman, unpublished observations), the morphogenetic effects of the loss of *FIG2* are less pronounced.

TABLE 1. Strains used in this study

Strain	Genotype	Source or reference
YSE20	*MAT***a** *ura3-52 leu2*Δ *his3*Δ *TRP1*	Y1407 (15)
YSE21	*MAT*α *ura3-52 leu2*Δ *HIS3 trp1*Δ	Y1408 (15)
YSE29	*MAT***a** *fig2*::*URA3 ura3-52 leu2*Δ *his3*Δ *TRP1*	Y1411 (15)
YSE30	*MAT*α *fig2*::*URA3 ura3-52 leu2*Δ *HIS3 trp1*Δ	Y1412 (15)
YSE332	*MAT***a** *aga1*::*URA3 ura3-52 leu2*Δ *his3*Δ *TRP1*	This study
YSE334	*MAT*α *aga1*::*URA3 ura3-52 leu2*Δ *HIS3 trp1*Δ	This study
YSE408	*MAT***a** *aga1*::*URA3 fig2*::*URA3 ura3-52 leu2*Δ *his3*Δ *TRP1*	This study
YSE409	*MAT*α *aga1*::*URA3 fig2*::*URA3 ura3-52 leu2*Δ *HIS3 trp1*Δ	This study
YSE430	*MAT***a** *ura3*Δ *leu2*Δ *his3*Δ *TRP1 met15*Δ *LYS2*	64
YSE431	*MAT*α *ura3*Δ *leu2*Δ *his3*Δ *TRP1 MET15 lys2*Δ	64
YSE548	*MAT***a** *fig2*::*KanR ura3*Δ *leu2*Δ *his3*Δ *TRP1 met15*Δ *LYS2*	64
YSE549	*MAT*α *fig2*::*KanR ura3*Δ *leu2*Δ *his3*Δ *TRP1 MET15 lys2*Δ	64

For assays of cell viability in the presence of mating pheromone, strains were grown overnight, and their densities were standardized to an optical density at 600 nm (OD_{600} of 0.4) as described previously (15). Cells were then treated with 10 μg of α-factor per ml (Sigma T6901) and removed at subsequent times for staining with methylene blue. Staining was done by adding methylene blue to final concentration of 0.001% and staining the cells with shaking at room temperature for 30 min. Following staining, cells were washed once in synthetic complete (SC) medium and immediately scored by microscopy at a magnification of ×100 for the fraction of cells staining. For each sample, at least 800 cells were scored. To examine cell viability in mating mixtures, cells were mated under the indicated conditions, after which, they were collected from the filters into SC medium and sonicated to disperse aggregated cells. Methylene blue was added to a final concentration of 0.001%, and the cells and zygotes were stained at room temperature for 30 min. We also quantified cell viability by measuring the colony-forming ability of cells plated to YPAD medium (yeast extract–peptone–dextrose [54] supplemented with 0.3 mM adenine) following treatments similar to a number of those described in the Results. The results of these experiments closely paralleled those we found by methylene blue assays. Cell fusion defects (partial and complete) were assayed by FM4-64 staining as described in reference 15.

Analyses of Pkc1 pathway activity by anti-MAPK immunoblot and reporter gene constructs. Yeast cells of the indicated strains and carrying the Slt2/Mpk1 gene on a high-copy, YEp24 plasmid were grown to mid-log phase at 30°C in synthetic complete medium lacking uracil (SC − ura). Cells were then diluted to an OD_{600} of 0.25 in fresh medium and allowed to grow until OD_{600} of 0.5 at 30°C before treatment with 10 μg of α-factor per ml at 24°C for 4 h. Cells were pelleted and transferred to an Eppendorf tube in 200 μl of cold morpholineethanesulfonic acid (MES) buffer (25 mM MES [pH 6.5], 10% glycerol, 100 mM NaCl, 100 mM KCl, 1 mM EDTA, 1 mM dithiothreitol, 5 mM NaF, 1 mM sodium orthovanadate, 20 mM β-glycerolphosphate, protease inhibitors). An equal volume of glass beads was added, and cells were lysed by vortexing. After

10 min of centrifugation at 4°C, supernatant of the extracts was collected. Laemmli buffer (15 μl) was added to 30 μl of extract, and the protein samples were denatured by heating at 95°C for 5 min and then separated on sodium dodecyl sulfate (SDS)–10% polyacrylamide gels. Western transfer to polyvinylidene difluoride Immobilon membranes was by semidry blotting. Blotted membranes were then preincubated for 1 h at room temperature in 1× PBST (PBS, 0.5% Tween 20) containing 5% nonfat dry milk. Following preincubation, the blot was incubated overnight at 4° in a 1/1,000 dilution of primary anti-p42/44 mitogen-activated protein kinase (MAPK) antibodies (New England Biolabs). The blot was then washed three times for 10 min each in 1× PBST and incubated for 2 h in the presence of a 1/4,000 dilution of a goat anti-rabbit horseradish peroxidase (HRP)-conjugated secondary antibody (Sigma). Detection of the HRP activity was by chemiluminescence via a Pierce SuperSignal detection kit. Blots were imaged by X-ray film or directly detected with a Kodak/NEN 440CF imaging system. Quantification of relative Mpk1 signals and total protein was determined with densitometry software associated with the Kodak/NEN 440CF imaging system. In the case of total protein, following development, the immunoblot was stained with Coomassie blue and imaged, and band intensities were integrated in each lane for all resolved proteins with the densitometry software.

To measure Rho1/Pkc1 pathway activity by Rlm1 binding site-driven *lacZ* reporter assay, cells of the indicated strains were transformed with a reporter plasmid, p2×Rlm1, or the parent, pLG178 (gifts of D. Levin) (22). Cells were grown SC − ura medium overnight and diluted into fresh YPAD medium at an OD_{600} of 0.1, after which they were allowed to double until they reached an OD_{600} of 0.4 to 0.5. Cells were then treated with 10 μg of α-factor mating pheromone per ml. Cells were harvested by centrifugation, washed 1× in Z buffer, and lysed and assayed for β-galactosidase activity as described in reference 15. The data presented represent the mean and standard error of three experiments.

Measurement of zygotic spindle alignment. Cells to be mated were grown, standardized for density, and mixed 1:1 in 18-mm-diameter culture tubes. One additional equivalent of fresh YPAD liquid medium was added (1 ml each of *MAT***a**, *MAT*α, and YPAD). Cells were mixed by vortex and immediately vacuum filtered onto a 0.45-μm-pore-diameter nitrocellulose filter (Millipore). Mating cells were placed onto solid media under the indicated conditions for 4 h. After mating, cells were recovered by washing from the filters into dropout medium supplemented with 0.1 volume of 10 mM adenine to suppress background fluorescence. Aggregates of mating cells were dispersed by sonication, and green fluorescent protein (GFP) fusion proteins were immediately visualized in the strains with a TE-300 microscope fitted with a ×100 Plan objective (Nikon) and GFP filter set (Chroma). Samples were not fixed or stored before viewing.

To quantify spindle alignment, zygotes viewed under the microscope were examined to determine the orientation of the Stu2::GFP fluorescence pattern. The orientation of this pattern with respect to the zygotic bud neck was determined. Any spindle showing one pole to have entered the bud, or the subsequent expansion of which was expected to project it through the bud neck, was scored as correctly aligned, while spindles whose ends were not expected to project into the bud based on their current orientation were considered incorrectly aligned. Zygotes with more than three disorganized and unaligned foci were considered separately. Nuclear position was also quantified by DIC or fluorescence microscopy of fixed wild-type and *fig2*Δ/*fig2*Δ zygotes that were prepared as described above, fixed, and stained with 4′,6′-diamidino-2-phenylindole (DAPI).

Measurement of agglutination. Agglutination assays of mating yeast cells were performed based on the method described by Terrance and Lipke (59) with the following modifications. *MAT***a** and *MAT*α cells were each grown separately in liquid medium at 30°C overnight. The cell cultures were standardized to an OD_{600} of 0.1 and grown for an additional 4 h at 30°C until they had reached an OD_{600} of 0.5. The *MAT***a** and *MAT*α cells and fresh medium were mixed 1:1:1 (2 ml each) and mated for 4 h at 30°C with constant mixing on a roller drum. The single cell types were also grown under the same condition for 4 h. All of the cell cultures were immediately fixed by adding 0.1 volume of 37% formaldehyde and allowed to fix either overnight at 4°C or for 1 h at room temperature. To measure the agglutination activity, 2.0 ml of fixed cell suspension was transferred into 4-ml cuvettes, and the cell aggregates were allowed to settle for 20 min. The two parent cell types were also measured as controls. The OD_{600} was measured with a spectrophotometer (Spectronic Genesys 8). The decrease in OD reading is a quantitative measure of agglutination. All samples were in triplicate. The agglutination index (AI) was calculated as $AI = 1 - [(2 \times A^{a+\alpha})/(A^{a} + A^{\alpha})]$ (59). For experiments involving sorbitol, matings were performed in liquid media with different sorbitol contents, and comparisons were made to the rate of settling of unmated cells in identical media.

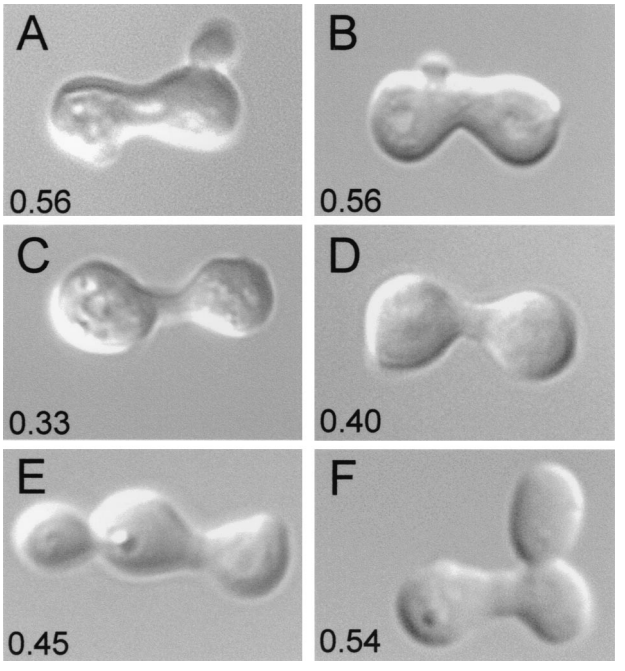

FIG. 1. Increased extracellular osmolarity suppresses the morphogenetic defect of *fig2*Δ cells. DIC images of representative wild-type and *fig2*Δ zygotes formed under the osmotic conditions indicated. The ratio of conjugation bridge/mean parental cell diameter is shown in the lower left portion of each image. Zygotes shown are from the following matings: YSE20 × YSE21 (*WT*), YPAD (A); YSE20 × YSE21 (*WT*), YPAD with 1.0 M sorbitol (B); YSE29 × YSE30 (*fig2*Δ), YPAD (C); YSE29 × YSE30 (*fig2*Δ), YPAD with 0.3 M sorbitol (D); YSE29 × YSE30 (*fig2*Δ), YPAD with 0.6 M sorbitol (E); YSE29 × YSE30 (*fig2*Δ), YPAD with 1.0 M sorbitol (F).

RESULTS

Mating morphogenesis defects of *fig2*Δ cells are osmotic remedial. Pheromone-induced morphogenesis is abnormal in mating mixtures of *fig2*Δ cells (15), and it is possible that the defects observed in these mutants result from altered cell wall structure or cell integrity signaling. Thin-section electron microscopy studies of the cell wall in the region of the mating projection previously showed this region to be thinner than the wall of vegetative cells (28). We therefore became interested in whether *FIG2* might be specifically expressed in mating cells to aid in organizing the region of the cell wall that is rapidly growing. Consistent with such a role, β-galactosidase fusions to an amino-terminal part of Fig2p and epitope-tagged forms of the protein have been localized to the mating projection (15, 18). To test whether the narrow mating projection and conjugation bridge phenotype previously observed in *fig2*Δ cells resulted from defects in processes that affected the integrity of the cell wall, we examined the responsiveness of the *fig2*Δ phenotype to conditions that osmotically stabilize the cell wall. Figure 1 shows the morphogenetic responses of wild-type (*WT*) and *fig2*Δ zygotes that result from mating cells on media differing only in osmolarity. Measurements of the width of the conjugation bridge in comparison to the mean parental width of zygotes previously showed that, in wild-type zygotes, this ratio is approximately 0.52, whereas in *fig2*Δ zygotes, the ratio is ~0.30 (15). Table 2 shows the mean values and standard

TABLE 2. Conjugation bridge morphogenesis in WT and *fig2*Δ zygotes

Zygote	Bridge diam/parental cell width in YPAD with the following concn of sorbitol[a]:			
	None	0.3 M	0.6 M	1.0 M
30°C				
WT × WT	55.6 ± 0.8	54.2 ± 0.9	53.7 ± 0.9	54.4 ± 1.0
*fig2*Δ × *fig2*Δ	34.6 ± 0.6	38.9 ± 0.8	45.5 ± 0.8	50.6 ± 0.8
37°C				
WT × WT	58.5 ± 1.6			56.4 ± 1.6
*fig2*Δ × *fig2*Δ	35.3 ± 0.9			45.1 ± 0.8

[a] Values represent ratios and associated standard errors of conjugation bridge diameter to mean parental cell widths for $n \geq 95$ zygotes, measured as described in Materials and Methods.

error obtained by making this comparison directly from images of over 100 zygotes for each pair of strains and mating condition. As is apparent from both Fig. 1 and Table 2, as osmotic conditions increase from 0.3 M sorbitol through 1.0 M sorbitol, the defects of *fig2*Δ mutants with respect to conjugation bridge morphogenesis are progressively more suppressed to a morphology very near that of wild-type zygotes. When conditions are isosmotic to hyperosmotic, all cells mate at reduced efficiencies (data not shown). Under these circumstances, *fig2*Δ cells, despite forming zygotes with similar morphologies to the wild type, encounter other problems affecting their mating success (described below). These data show that the *fig2*Δ morphogenetic defects are suppressible by conditions that have previously been reported to compensate for defects in cell wall biogenesis or structure (26, 40, 48).

FIG2 is also required for normal cell-cell fusion during mating. A number of different genes encoding cell polarity proteins and necessary for efficient mating cell fusion play roles in both vegetative and mating cell morphogenesis (e.g., *SPA2*, *BNI1*, *KEL1*, and *PEA1*) (reviewed in reference 63). Thus, the defects in cell fusion seen in *fig2*Δ matings might be a direct result of morphogenesis defects. Alternatively, the mating cell fusion defects might reflect a role of *FIG2* in this process that is independent of its morphogenesis functions. To address this question, we examined the fraction of cells in the different matings in the experiments just described that existed as coupled cells (prezygotes) or zygotes and noted any defects in cell fusion processes. As Fig. 2 and Table 3 illustrate, *fig2*Δ cells mated on YPAD medium show an approximate twofold increase in the fraction of zygotes showing defects in cell fusion,

TABLE 3. Cell fusion defects in WT and *fig2*Δ/*fig2*Δ zygotes

Zygote	% of cells with defects[a]			
	30°C		37°C	
	YPAD	YPAD–1 M sorbitol	YPAD	YPAD–1 M sorbitol
WT × WT	5.3	4.0	11.3	12.0
*fig2*Δ × *fig2*Δ	12.3	10.6	23.8	20.0

[a] Values represent percentages of $n \geq 150$ paired conjugating cells (prezygotes and zygotes) displaying partially or completely unfused cells as visualized by FM4-64 and DAPI staining (15). The mating mixtures assayed were the same as those presented in Table 2.

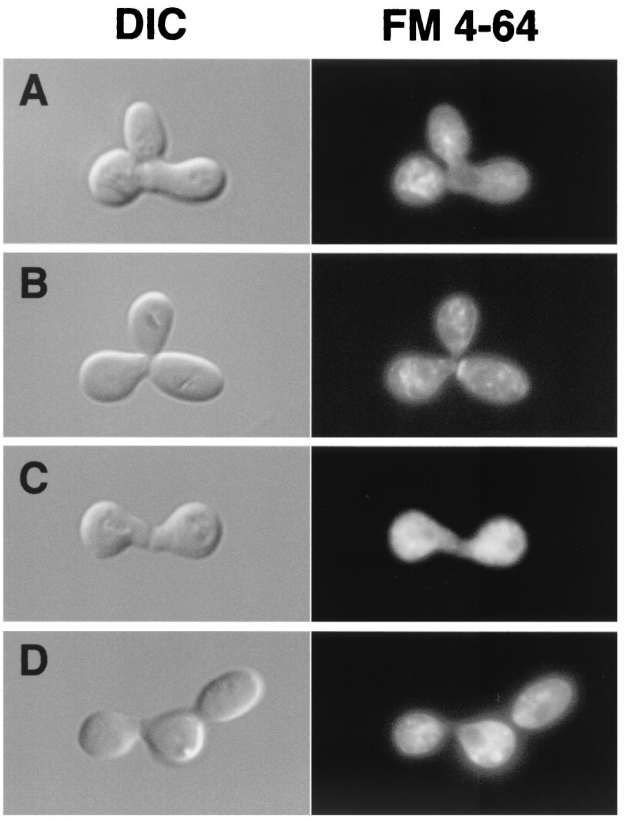

FIG. 2. Suppression of *fig2*Δ/*fig2*Δ zygote phenotypes by increased osmolarity acts specifically on morphogenetic and not cell-cell fusion defects. DIC and FM4-64-stained fluorescence images of zygotes formed in matings carried out in YPAD–1.0 M sorbitol medium. Micrographs are of A) YSE20 × YSE21 (*WT*) (A) and (panels B, C, and D) YSE29 × YSE30 (*fig2*Δ) zygotes display sorbitol-suppressed, normal conjugation bridge morphogenesis, but remain defective in cell fusion.

as previously reported (15). However, in contrast to the results obtained with respect to suppression of the narrow conjugation bridge phenotype, changes in external osmolarity failed to rescue defects of *fig2*Δ mating cells in the cell fusion process. These results suggest that the requirements for *FIG2* in mating cell morphogenesis and cell fusion can be uncoupled by osmotic conditions and therefore are likely to be in some way distinct.

High temperature interferes with the osmotic suppression of *fig2*Δ and cell fusion. Given that sorbitol suppressed defects of *fig2*Δ cells in mating cell morphogenesis, and since Rho1 and Pkc1 participate in both cell integrity signaling and polarized cell growth, we further investigated whether elevated signaling by the Rho1/Pkc1 pathway might be responsible for some of the phenotypes observed in *fig2*Δ cells. We again carried out the preceding experiments, except that cells were mated at an elevated temperature, 37°C, which has been shown to activate signaling through the Rho1/Pck1 pathway (23). Table 2 shows the results of these experiments in comparison to matings carried out at 30°C with respect to sorbitol suppression of conjugation bridge morphogenesis defects present in *fig2*Δ zygotes. These data indicate that while elevated temperature does not significantly enhance the baseline effect of *fig2*Δ in the

absence of osmotic support, high temperature does reduce the extent to which sorbitol suppresses the effects of *fig2*Δ on conjugation bridge morphogenesis (Table 2). We also examined cell fusion in these experiments and observed a twofold increase in cell fusion defects when cells of all genotypes are mated at 37°C (Table 3).

Conditions of elevated temperature and polarized growth during mating activate the Rho1/Pkc1 pathway (4, 23, 47, 65). Our data indicate that loss of *FIG2* also increases signaling through this pathway during mating (described below). One interpretation of these results is that the combination of these three conditions (mating, high temperature, and loss of *FIG2*) produces a level of signaling in this pathway that can no longer be suppressed by the osmotic quenching of pathway signaling that can occur under vegetative conditions (23).

FIG2* is required for the maintenance of cell integrity during mating.** A number of gene products have been shown to be required for maintenance of the viability of cells during mating, including the *MID2* gene product, which functions as a sensor upstream of the Rho1/Pkc1 pathway (24, 41, 45). A potential role for Fig2p in organizing components of the mating cell wall would predict that the absence of the protein during mating might lead to diminished integrity of cells due to defects in wall organization. We therefore tested whether *fig2*Δ strains were less viable than wild-type cells after the onset of mating cell morphogenesis. Two types of assays were employed to quantify viability under different conditions to test mating cell function. We first tested whether treatment of *MATa** cells with levels of α-factor mating pheromone that elicit mating cell morphogenesis, and which have previously been shown to reveal defects in cell integrity for other mutants, would reveal viability differences between wild-type and *fig2*Δ cells under such conditions. The fraction of cells staining with the dye methylene blue, which is excluded from viable cells, was examined immediately following pheromone treatment at the times indicated in Fig. 3A. Cells from two different strain backgrounds were examined, and the results of both show that, relative to wild-type cells, *fig2*Δ cells are markedly reduced in viability following extended treatment with morphogenesis-inducing levels of mating pheromone. This reduction in viability was not accentuated by removal of Ca^{2+} from the medium by addition of EGTA, nor was it suppressed by addition of Ca^{2+} to levels up to 100 mM (data not shown). Thus, the effect of *fig2*Δ on cell viability does not appear to occur through blocking of the essential transport of Ca^{2+} ions into mating cells (21, 35).

We next sought to determine whether *fig2*Δ cells displayed reduced viability under actual mating conditions and whether zygotes or nonmating cells displayed differential sensitivities. For these studies, *MAT***a** and *MAT*α cells were mated on filters for a period of 4 h, after which, the fraction of methylene blue-stained cells was determined by microscopy. Figure 3B, C, and D show the results of these studies, which indicate that *fig2*Δ cells are significantly less viable than wild-type cells in mating mixtures under nearly every condition tested. Figure 3B and D show that as osmolarity levels of 0.6 M sorbitol and above are encountered, *fig2*Δ cells can be seen to show a sharp reduction in viability relative to wild-type cells. Interestingly, when zygote formation was quantified in these experiments (Fig. 3C), we found that there was a significant decrease in the rate of zygote formation of *fig2*Δ cells under hypoosmotic mating conditions, but this inhibition was alleviated by elevated osmolarity. However, while elevated osmolarity leads to increased zygote formation in such cells, a large fraction of such *fig2*Δ zygotes are inviable (Fig. 3D). In each of the assays described above, analyses of the responses of vegetative cells to elevated osmolarity conditions showed no difference in viability or growth rate of *fig2*Δ cells in comparison to wild-type strains, consistent with the induced expression and known roles of *FIG2* in mating. In summary, the effects of *fig2*Δ mutations on mating cell viability in both α-factor-treated cells and in mating mixtures suggests a common defect in the maintenance of cell integrity that cannot be rescued by elevated levels of osmotic support.

Rho1/Pkc1 pathway activity is elevated in *fig2*Δ cells undergoing mating morphogenesis. Our data concerning morphogenesis, cell fusion, and cell integrity defects of *fig2*Δ mutants suggested the hypothesis that the Rho1/Pkc1 cell integrity pathway might be activated in such cells in a manner inappropriate to its normal signaling functions in mating. The Rho1/Pkc1 pathway has previously been shown to undergo activation in response to pheromone-induced morphogenesis (4, 47). To test our hypothesis, we first examined whether Mpk1p/Slt2p, the MAPK that lies downstream of Pkc1p in its signaling pathway, was activated to higher levels in *fig2*Δ cells undergoing mating cell morphogenesis than it normally is in wild-type cells. Wild-type and *fig2*Δ *MAT***a** cells were treated with morphogenesis-inducing levels of mating pheromone for 4 h, after which, the cells were harvested by centrifugation and lysates were prepared. Protein extracts were electrophoresed on SDS-polyacrylamide gel electrophoresis (PAGE), and were semidry transferred to nylon membrane and then incubated with anti-p42/44 MAPK antibodies that preferentially recognize the phosphotyrosine form of MAPKs. This antibody has been used by others successfully to detect the MAPK Mpk1p/Slt2p and is specific to the activated, tyrosine-phosphorylated form of the MAPK (S. Vidan and M. Snyder, personal communication). As shown in Fig. 4 A, by detecting both the endogenous Mpk1p/Slt2p and the protein present in cells, where it is encoded endogenously and on a high-copy plasmid, YEp24-*MPK1*/*SLT2* (12), we observed increased levels of activated Mpk1p/Slt2p in *fig2*Δ cells relative to wild-type cells. Scanning densitometry of the films and normalization of signals to lane loading of total protein indicates that Mpk1p/Slt2p is found at 3.5- to 24.0-fold the levels in mating pheromone-treated *fig2*Δ cells relative to wild-type cells. These data therefore support the hypothesis that the absence of Fig2p from the mating cell wall leads to a further increase in Rho1/Pkc1 pathway activity. This level of Mpk1p activation may be inappropriately high for mating cells and thereby cause the morphogenesis, cell fusion, and zygotic spindle alignment defects (see below) associated with *fig2*Δ cells.

We used a second approach to independently assess Mpk1p/Slt2p activation levels in *fig2*Δ cells in comparison to wild-type cells. Plasmids carrying either a *cyc1-lacZ* reporter gene lacking UAS sequences alone, pLG, or with two upstream Rlm1 binding sites, p2×Rlm1, were transformed into the strains we had examined for Mpk1p activation. Rlm1p is a DNA binding transcriptional activator that lies directly downstream of Mpk1p, and its activity is directly controlled by the Pkc1≫Mpk1 sig-

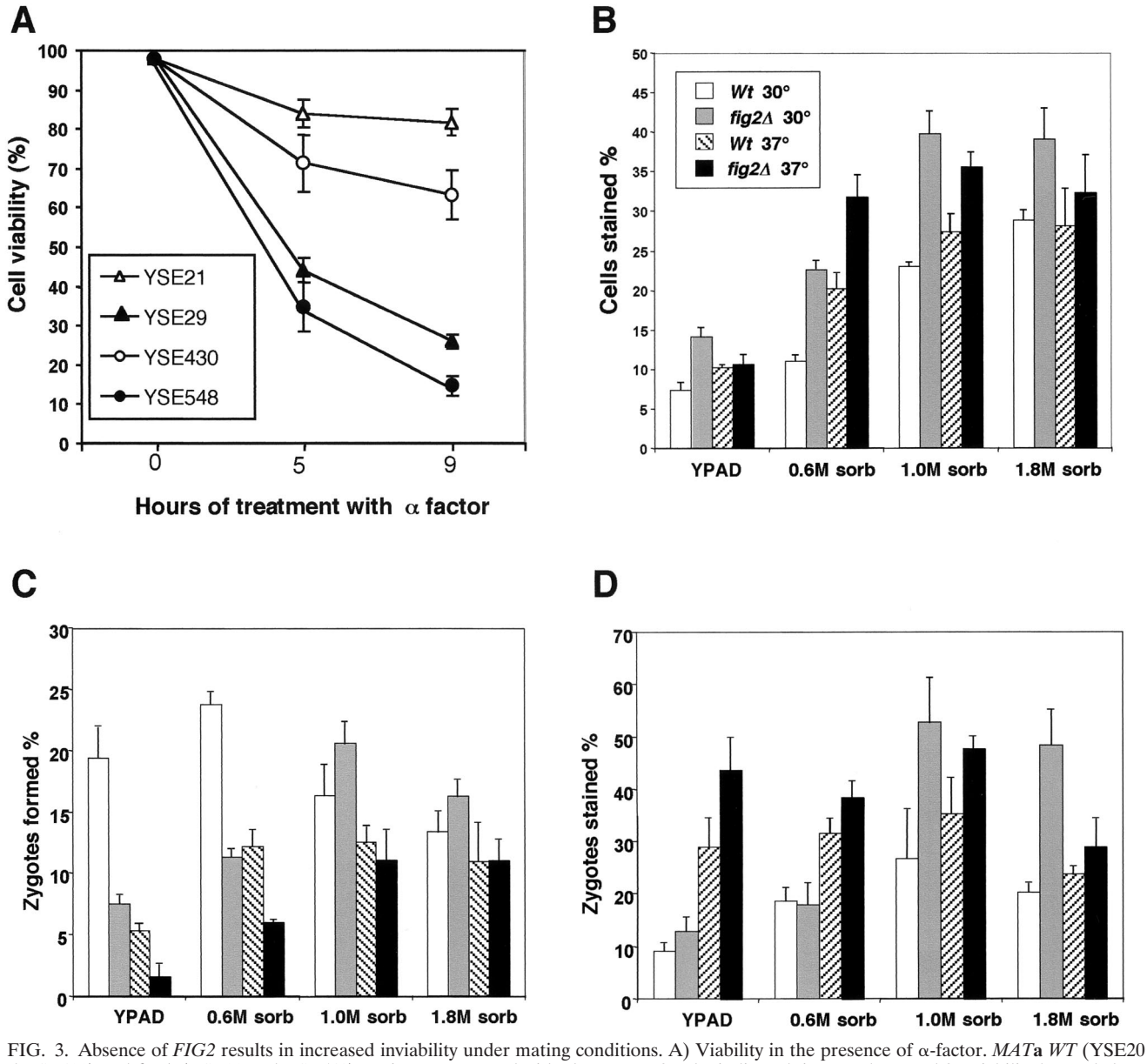

FIG. 3. Absence of *FIG2* results in increased inviability under mating conditions. A) Viability in the presence of α-factor. *MAT***a** *WT* (YSE20 and YSE430) and *fig2*Δ (YSE29 and YSE548) strains were treated with pheromone for the indicated times and assayed for viability by methylene blue exclusion. (B) Mating cells from bilateral crosses of *Wt* (YSE21 × YSE22) and *fig2*Δ (YSE29 × YSE30) strains were assayed for viability by methylene blue exclusion immediately following mating for 4 h on solid media under the conditions indicated. Values represent percentages from over 800 cells counted. (C) Zygote formation rates for the crosses indicated in panel B. (D) Viability of zygotes in mating mixtures shown in panel B.

naling pathway. This reporter plasmid has previously been shown to be induced 6.5- to 16.5-fold after 4 h under different conditions of cell wall stress (U. S. Jung and D. Levin, personal communication). *MAT***a** wild-type and *fig2*Δ strains carrying these plasmids were grown in liquid culture, and cells were treated with morphogenesis-inducing levels of α-factor pheromone for 4 h. Following pheromone treatment, cells were assayed for β-galactosidase activity as described in Materials and Methods. As Fig. 4B shows, wild-type and *fig2*Δ strains carrying the 2×Rlm1 reporter both show an α-factor-dependent increase in activity. In *fig2*Δ cells, however, there is an elevation of basal signaling in the absence of α-factor (~2.2-fold) and a marked elevation under conditions of α-factor induction (~3.6-fold). These data are in close agreement with the relative increases we found in pathway signaling as measured by immunoblot comparison of endogenous Mpk1p/Slt2p activation (3.5-fold). In summary, these experiments assessing Mpk1p and Rlm1p activity levels show that signaling through the Rho1/Pkc1 cell integrity pathway occurs at significantly elevated levels in *fig2*Δ cells relative to those in wild-type cells during mating.

Zygotic spindle alignment requires *FIG2* function. Initial studies of *fig2*Δ × *fig2*Δ matings noted an unusual appearance and possible mislocalization of the nucleus in zygotes formed in these crosses, as visualized by DAPI staining (15). We sought to further investigate whether nuclear migration is al-

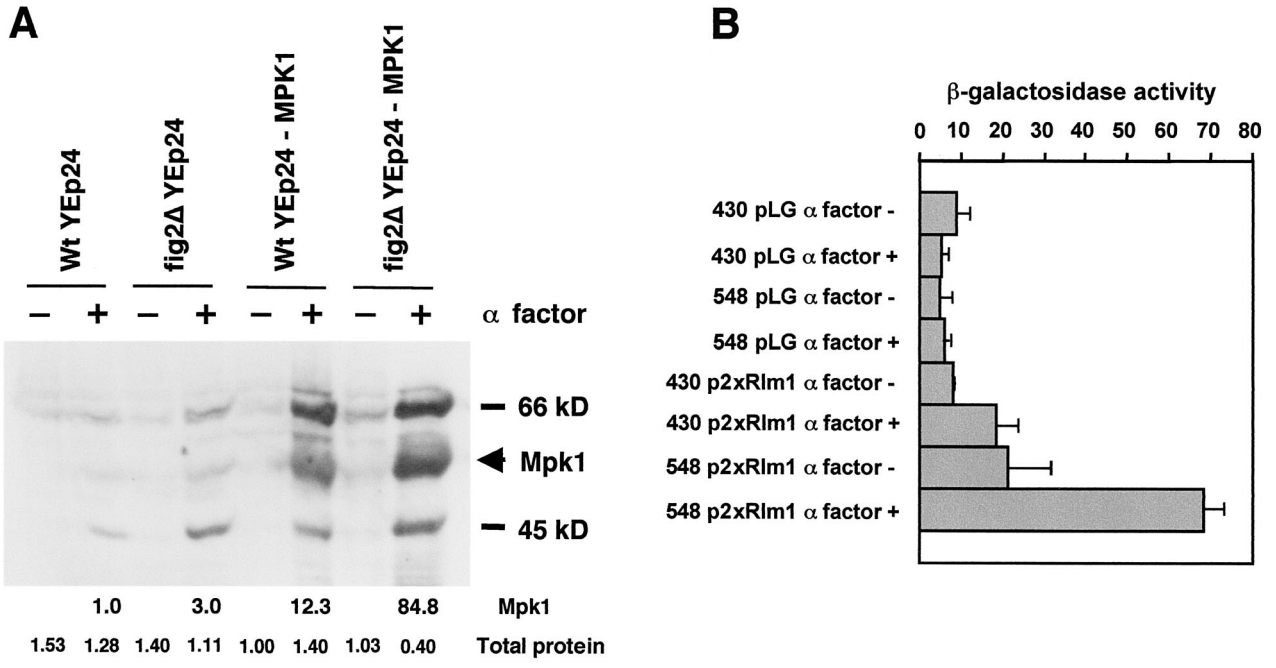

FIG. 4. Activation levels of the Rho1/Pkc1 cell integrity pathway are greater in *fig2*Δ cells than in the wild type. (A) Anti-MAPK immunoblot detecting activation of Mpk1p following pheromone treatment in YSE430 (*WT*) and YSE548 (*fig2*Δ) cells carrying the plasmid YEp24 or the same cells each carrying the plasmid YEp24-MPK1/SLT2. Numbers below the lanes indicate the relative intensity of Mpk1 in each lane and relative total protein levels determined as described in Materials and Methods. (B) Activity levels of the Pkc1 pathway assayed by a 2×Rlm1 binding site-dependent β-galactosidase reporter, p2×Rlm1 in YSE430 (*WT*) and YSE548 (*fig2*Δ) cells following mating pheromone treatment. pLG is the parent *cyc1-lacZ*-containing vector, which contains no Rlm1 binding sites.

tered in such cells and whether this phenotype is influenced by osmotic conditions. To quantify nuclear migration in zygotes, we transformed *MAT***a** and *MAT*α wild-type and *fig2*Δ cells with a centromere-based plasmid carrying a Stu2::GFP fusion gene (61). The encoded Stu2::GFP fusion protein localized to spindles and spindle pole bodies in wild-type cells as previously reported. Spindle localization was seen as a bar of staining as shown in Fig. 5A to D. In zygotes that had initiated a bud, we quantified the alignment of the spindle axis with respect to the mother (zygote)-bud axis as described in Materials and Methods. Table 4 shows that spindles are aligned with the zygote-bud axis approximately 18% less well in *fig2*Δ zygotes than in wild-type zygotes. Because we found that osmotic support suppressed morphogenesis defects in such zygotes, we tested whether a similar suppression was possible for the spindle alignment defect. Table 4 shows that conditions that can compensate for cell wall stress and reduce Pkc1 pathway signaling (1.0 M sorbitol) also suppress 61% of the difference in spindle alignment fidelity seen between wild-type and *fig2*Δ cells. These data also show that the process of spindle alignment in *fig2*Δ/*fig2*Δ zygotes is more sensitive to cold than it is in wild-type zygotes. These data, obtained with strains from this independent S288C background (YSE548 and YSE549), agree with previous findings that *fig2*Δ × *fig2*Δ matings are markedly cold sensitive in comparison to the wild type (15). To further confirm our observations concerning spindle alignment and nuclear positioning, we also scored by DIC or fluorescence microscopy of DAPI-stained cells the locations of single, fused zygotic nuclei in zygotes that had initiated a bud that had grown to medium to mature size. Zygotes were divided into the following three classes: I, nucleus present in either parent of the zygote; II, nucleus present in the bridge of the zygote near the zygote-bud neck; and III, nucleus present completely in the bud. The distributions of these classes for wild-type zygotes were I = 2.0%, II = 93%, and III = 5% (n = 204 zygotes scored), and the distributions in *fig2*Δ/*fig2*Δ zygotes were I = 7.6%, II = 85.7%, and III = 6.7% (n = 207 zygotes scored). Collectively, these data indicate that spindle positioning by astral microtubule dynamics in zygotic divisions is impaired in *fig2*Δ/*fig2*Δ zygotes. These defects and the morphogenesis defects in *fig2*Δ cells and zygotes may therefore occur through a common mechanism.

In *fig2*Δ/*fig2*Δ zygotes, we also noted another difference in Stu2::GFP localization relative to wild-type cells, such that 4.3% of all zygotes examined in *fig2*Δ × *fig2*Δ mating mixtures contained patterns of Stu2::GFP localization to a small number of distinct foci, as shown in Fig. 5E and F, in comparison to 1.1% observed in matings of wild-type cells ($n \geq 280$). These foci occurred in clusters in cells and were not located near presumptive sites of spindle poles. Cells displaying these foci of Stu2::GFP were rarely observed in wild-type mating mixtures, and this localization was not strictly correlated with the stage of cells in mating with respect to their being unbudded, polarized, or a zygote, although the frequency of foci was somewhat higher in zygotes relative to the other classes. When cells were mated on media containing 1 M sorbitol, foci were observed in only 1.3% of *fig2*Δ/*fig2*Δ zygotes and 0.6% of wild-type zygotes ($n \geq 150$). These data indicate that the mislocalization of Stu2p in *fig2*Δ zygotes is also substantially suppressed by increases in extracellular osmolarity.

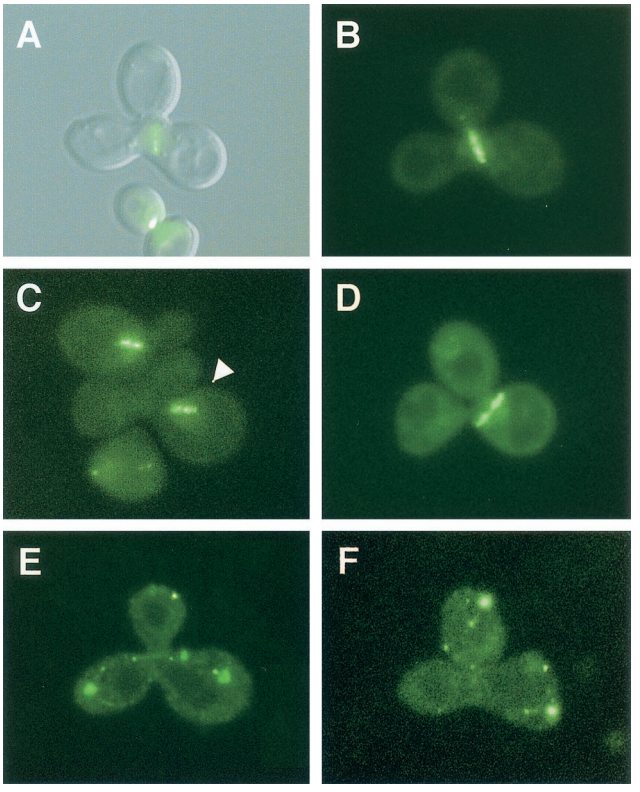

FIG. 5. Reduced zygotic spindle alignment fidelity and mislocalization of the spindle/microtubule-associated protein Stu2p in *fig2*Δ/*fig2*Δ zygotes. (A) Merged DIC-GFP fluorescence images of Stu2::GFP fusion proteins decorating a wild-type aligned spindle. (B, C, and D) GFP fluorescence images of wild type aligned (B), and *fig2*Δ/*fig2*Δ unaligned (C and D), zygotic spindles. (E and F) GFP fluorescence images of Stu2::GFP fusion proteins incorrectly mislocalized to discrete foci in *fig2*Δ/*fig2*Δ zygotes.

Enhanced agglutination of *fig2*Δ cells during mating depends on agglutinins. Cells lacking *FIG2* show increased agglutination in bilateral matings under liquid conditions (15), and when *FIG2* is ectopically expressed in vegetative cells, cell-cell adherence is modified (18). To help understand the basis of the enhanced agglutination observed in matings involving *fig2*Δ cells, we further investigated its mechanism. Figure 6 shows again that agglutination is most strongly enhanced when both mating partners are missing *FIG2*. However, in unilateral matings in which only one partner is *fig2*Δ, increased agglutination occurs only in the context in which the *fig2*Δ cells are the *MAT*α partner. This is evident by the strong agglutination of *wt* × *fig2*Δ matings in comparison to *fig2*Δ × *wt* and bilateral crosses of *wt* and *fig2*Δ strains alone (Fig. 6). Thus, the mechanism of *FIG2* modulation of agglutinin activity is largely α partner specific, although its absence from both partners does lead to maximally increased agglutination. This suggests an additional interaction with a non-cell-type-specific component of the process. Similar results concerning this mechanism have also recently been found by others (C. Jue and P. Lipke, personal communication)

TABLE 4. Zygotic spindle alignment in WT and *fig2*Δ zygotes

Zygote	% Aligned[a]		
	30°C		16°C YPAD
	YPAD	YPAD–1M sorbitol	
WT/WT	89.4	92.0	83.2 (0.93)
*fig2*Δ/*fig2*Δ	71.4 (0.79)	82.7 (0.89)	61.2 (0.86)

[a] Values represent percentages based on $n \geq 150$ zygotes examined; numbers in parentheses indicate the fraction of WT spindle alignment fidelity occurring at 30°C represented by the given value.

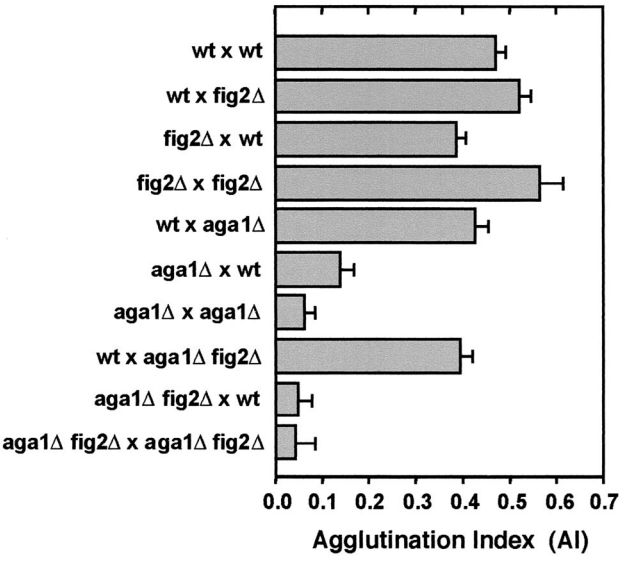

FIG. 6. Enhanced agglutination due to loss of Fig2p is dependent upon the mating agglutinins. Agglutination indices are shown for bilateral matings of wild type and *fig2*Δ cells, as well as reciprocal unilateral crosses involving wild-type, *aga1*Δ and *aga1*Δ *fig2*Δ strains.

FIG2 and *AGA1* encode GPI-anchored proteins that share sequence homology in regions containing WCPL domains and a CX $_4$C domain (53; M. Zhang and S. Erdman, unpublished data). These genes have also recently been found to be collectively important for some aspect of efficient mating that is independent of the agglutinin Aga2p (18). To determine whether the mechanism of enhanced agglutination induced by *fig2*Δ strains operated through the agglutinins Aga1p, Aga2p, and Agα 1p, we tested the ability of *fig2*Δ to enhance the agglutination of cells carrying *aga1*Δ mutations. As shown in Fig. 6, the effect of *fig2*Δ is largely dependent on interactions between the agglutinins, as evidenced by strongly reduced agglutination in *MAT***a** *aga1*Δ *fig2*Δ double mutants.

Increased osmolarity fails to reduce enhanced agglutination due to loss of *FIG2*. Because sorbitol was effective in suppressing other defects associated with loss of *FIG2*, we sought to determine whether osmotic support could compensate for the agglutination effects observed in the absence of *FIG2*. To test this, we compared the agglutination behavior of *fig2*Δ mutants to that of wild-type cells mated under different osmotic conditions. As Table 5 shows, under conditions of elevated extracellular osmolarity, while cells of every genotype tested agglutinate much less, particularly at sorbitol concentrations of 0.6 M and above, there is no specific elimination of the enhanced agglutination of *fig2*Δ cells relative to wild-type cells. These data demonstrate that the effects of *fig2*Δ on agglutination are

TABLE 5. Effects of osmolarity on the enhanced agglutination of *fig2*Δ cells[a]

Cell type	AI	% Reduction due to sorbitol
WT × WT	0.48 ± 0.02	
YPAD–0.3 M sorbitol	0.36 ± 0.02	24
YPAD–0.6 M sorbitol	0.21 ± 0.01	57
YPAD–1.0 M sorbitol	0.22 ± 0.01	54
*fig2*Δ × *fig2*Δ	0.58 ± 0.03	
YPAD–0.3 M sorbitol	0.51 ± 0.03	12
YPAD–0.6 M sorbitol	0.34 ± 0.01	41
YPAD–1.0 M sorbitol	0.31 ± 0.03	46

[a] Values represent AI measurements from three independent experiments as described in Materials and Methods for WT (YSE21 × YSE22) and *fig2*Δ (YSE29 × YSE30) strains.

independent of the osmolarity of the medium. Thus, the phenotypic effects of *fig2*Δ mating cells with regard to morphogenesis, cell integrity, and spindle positioning are evidently separable from those involving agglutination.

DISCUSSION

In the present study, we describe new roles for *FIG2* in the maintenance of mating cell integrity and zygotic spindle alignment and further examine the nature of different phenotypic effects of *fig2*Δ mutations in the yeast mating process. These studies suggest a complex interplay between pheromone signaling and its downstream targets, including *FIG2* and signaling pathways maintaining cell integrity. These pathways are likely to be related through both dependent relationships and feedback loops that are active under different physiological conditions.

Cell wall organization through Fig2p underlies several mating processes. *FIG2* is one of many genes whose induced expression occurs by activated mating pathway signaling and which serve to differentiate cells, enabling them to efficiently carry out the mating process (15, 31, 56). Studies thus far have described both negative and positive roles for *FIG2* in mediating cell adhesion processes (15, 18; C. Jue and P. Lipke, personal communication). One apparent positive role for Fig2p occurs in the absence of another adhesin, Aga1p, and is independent of Aga2p, the functional portion of the *MAT***a** cell agglutinin molecule (18; S. Erdman, unpublished observations). Currently, it remains unclear what this Aga1p-related and agglutination-independent role may be, although it has been observed that few *fig2*Δ *aga1*Δ cells are found to be mating in mating mixtures (18; S. Erdman, unpublished observations). Additional roles for *FIG2* in cell-cell fusion and spatial control of morphogenesis during mating have been described previously (15). Here, we have identified additional positive functions for *FIG2* in mediating survival of mating cells and in aiding the fidelity of the alignment process that zygotic spindles undergo.

The involvement of Fig2p in the multiple processes of cell adhesion, cell-cell fusion, cell morphogenesis, cell integrity maintenance, and zygotic spindle alignment prior to anaphase suggests that some of these defects may be secondary effects due to the loss of *FIG2*. Because Fig2p is located outside of the cell, it follows that the morphogenesis and zygotic spindle-positioning functions of Fig2p must be indirect and therefore involve transmembrane signaling. Of the remaining processes that require Fig2p, regulation of agglutination and maintenance of cell integrity, the effects on agglutination might also be indirect due to general alterations in the structure of the cell wall caused by the absence of Fig2p. The absence of Fig2p might alter mating cell wall organization, making the agglutinins more accessible, or loss of *FIG2* might reduce competition for anchor attachment machinery that could arise among the GPI-anchored adhesin proteins Aga1p, Agα 1p, and Fig2p during their biogenesis. These aspects of the *fig2*Δ phenotype involving cell adhesion control remain to be addressed.

Our results demonstrate that *fig2*Δ cells are less viable relative to wild-type cells under conditions promoting mating cell morphogenesis and in response to prolonged mating pathway activation. Because Fig2p is a cell wall resident protein, it seems logical that a major and primary role for Fig2p in cells is to help modulate and organize cell wall structure in the region of the mating projection where it is localized. Fig2p may function directly to organize other cell wall resident mannoproteins or the cell wall (glucans and chitin) itself. This type of organizational role might be critical to the maintenance of cell wall structure and therefore cell integrity during the rapid cell wall remodeling events accompanying projection growth and cell-cell fusion during mating. These requirements would be expected to be even more important to mating cells that experience changes in their environment in regard to external osmolarity. Such a function for Fig2p is consistent with several observations. Ultrastructural studies of the mating projection have demonstrated the thinned and differentiated nature of the cell wall in the region of the tip of the projection (28). Studies demonstrating chitin synthase induction by pheromone and chitin localization to polarized growth sites in the region of the mating projection are also consistent with the need to maintain integrity in this region of the cell (1, 5, 50). It has also been observed that mutations such as *mpk1*Δ and *swi4*^{ts} that lead to fragile cells cause lysis at this site during morphogenesis (26, 29, 40). Thus, we posit that a key role *FIG2* plays is in the maintenance of mating cell integrity.

Control of Rho1/Pkc1 cell integrity signaling is essential to normal mating. A regulatory role of the Rho1/Pkc1 pathway governing cell-cell fusion has been previously described, and our data further support this hypothesis (42). The frequency of cell fusion defects observed in the absence of *FIG2* (twofold) is relatively close to that reported to occur under conditions of excess Rho1/Pkc1 activity due to a dominant active *PKC1-R398P* allele (eightfold; shown in row 2 in Table 6 in reference 42). The magnitudes of these effects are consistent with loss of *FIG2* creating a partial activation of this cell fusion blockade due to elevated Rho1/Pkc1 activity. We found that *fig2*Δ defects in cell fusion were not suppressible by 1 M sorbitol, whereas Philips and Herskowitz (42) found that *PKC1-R398P*-mediated defects were partially osmoremedial. One interpretation of these different results is that cell fusion functions requiring *FIG2* represent part of the remaining fraction of osmolyte-insensitive cell fusion defects they observed. Under both of these conditions, elevated Rho1/Pkc1p activity may still remain, preventing or significantly delaying some prezygotes from completing mating cell fusion. We note that this effect of

Fig2p on cell fusion does not preclude the possibility that Fig2p might also function more directly during cell fusion to facilitate cell-cell contact and adhesion.

The Rho1/Pkc1 cell integrity pathway has recently been shown to act in G_2 to help coordinate a morphogenesis checkpoint that aids damaged, shocked, or defective cells in accurately completing bud growth and the cell cycle (19). In addition, its activities in response to defective polarized growth and cell wall assembly are well established (reviewed in references 17, 43, and 62). Studies have clearly demonstrated roles for pathway components in polarized growth of mating projections and the maintenance of mating cell integrity, placing them in good position to act as regulators as well (12, 13, 29, 30). In further support of this function we found evidence that Mpk1p/Slt2p, the MAPK controlled by Rho1/Pkc1 signaling is more abundant and active in *fig2*Δ cells exposed to mating pheromone than in wild-type cells.

Mating processes dependent on Fig2p have distinct requirements for its function. We observed that defects in some of the processes dependent upon *FIG2* are remedial in *fig2*Δ cells when extracellular osmotic support is provided, while for other functions, this relationship does not hold. Mating cell morphogenesis and zygotic spindle alignment can be rescued by elevated osmolarity, while cell-cell fusion, agglutination control, and cell integrity differences in *fig2*Δ cells remain unaffected by changes in osmolarity. Further studies involving *mid2*Δ *fig2*Δ double mutant strains have provided additional evidence that the phenotypes arising due to the absence of *FIG2* are distinct. *MID2* encodes a sensor for Rho1p that functions during mating (24, 41); deletion of this gene would be expected to suppress aberrant signaling to Rho1p caused by the absence of Fig2p. Our analysis of zygotic spindle positioning in zygotes formed in bilateral matings of *mid2*Δ *fig2*Δ double mutant strains shows that the frequency of misaligned spindles is indistinguishable from that in wild-type cells (~11%, $n = 150$ zygotes). At the same time, *mid2*Δ *fig2*Δ cells still possess agglutination phenotypes characteristic of *fig2*Δ strains, again showing the separable nature of *fig2*-dependent effects. Collectively, these data suggest that the roles of Fig2p in these processes are distinct activities of the protein. Alternatively, differential requirements may exist for the level of Fig2p activity in these processes, which, for example, can be rescued for such processes as morphogenesis, but remain insufficient for others that require greater levels of activity, such as cell fusion. Continued study of Fig2p and its roles in these processes should help elucidate the nature of these requirements.

We believe that several *FIG2*-dependent mating processes that are responsive to Rho1/Pkc1 signaling are likely to be related in a manner shown in the model presented in Fig. 7. In the absence of *FIG2*, mating cell wall assembly is aberrant, and Rho1/Pkc1 signaling is elevated, as shown in the lower half of the model. This elevation in Rho1/Pkc1 signaling normally reduces the rate of cell wall erosion and cell fusion, instead maintaining increased assembly of the wall through glucan synthase effectors of Rho1p, which are also likely to be activated under these conditions (32, 44). These delays in cell fusion may then translate into prolonged projection morphogenesis and delays in subsequent lateral expansion of the conjugation bridge, a process that occurs shortly following cell fusion in both *S. cerevisiae* and *Schizosaccharomyces pombe* (8, 16). Such changes in the normal program of polarized cell growth during mating would be expected to produce the narrow mating projection and conjugation bridge associated with the absence of *FIG2* from mating cells and zygotes in certain strain backgrounds. Consistent with such a model, elevated temperature conditions, which activate the Rho1/Pkc1 pathway, were also found to increase cell fusion defects and to reduce the efficacy of sorbitol suppression of conjugation bridge morphogenesis defects occurring in the absence of *FIG2*. Osmotic support strongly reduces signaling through the Rho1/Pkc1 pathway (23) and suppresses defects in conjugation bridge morphogenesis and in spindle positioning (this study). Under such conditions, it may be that a checkpoint blocking normal conjugation bridge morphogenesis and expansion is relieved without removing the defect due to absence of Fig2p, and hence the fusion defects remain under these conditions. Alternatively, conjugation bridge morphogenesis and spindle positioning may be independently affected by high Rho1/Pkc1 activity levels in a manner that, unlike the mechanism controlling cell fusion, can be effectively relieved by increased osmolarity.

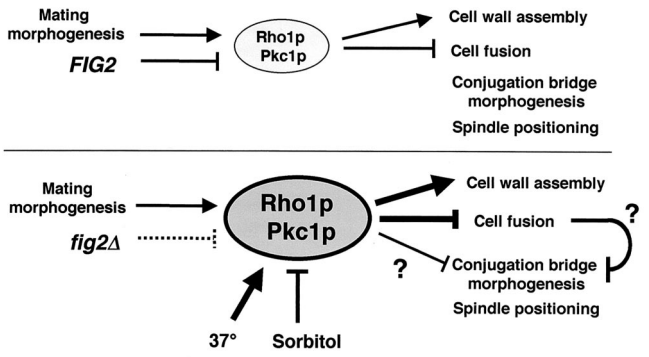

FIG. 7. Model of *FIG2* function in mating morphogenesis, cell fusion, and cell integrity. In wild-type cells, Fig2p is deposited in the cell wall during and throughout mating cell morphogenesis. Polarized growth activates Rho1/Pkc1 signaling, increasing cell wall assembly in the projection area and delaying cell fusion until a partner is sensed. Once activated Rho1/Pkc1 levels fall and cell fusion begins, lateral expansion of the conjugation bridge and subsequent spindle positioning occurs. In *fig2*Δ cells, Fig2p is absent from the mating cell wall, leading to its disorganization or perhaps increased pressure in the region of the projection where Fig2p is normally present. This change is signaled, leading to more elevated Rho1/Pkc1 activity. This higher level of activity normally feeds back to enhance cell wall biogenesis, partially compensating for absence of Fig2p. Elevated activity nonetheless leads to delays in cell fusion and spindle position and may delay lateral morphogenesis of the conjugation bridge. Conditions of higher temperature or sorbitol support enhance or suppress these phenotypes, respectively, through their effects on Rho1/Pkc1 signaling.

One question that remains is why cells lacking *FIG2* are not osmoremedial for their defects in cell integrity during mating. It is likely that in *fig2*Δ cells, a reduction in signaling through Rho1/Pkc1 via sorbitol reduces cell wall assembly by glucan synthase effectors of Rho1p. Because such cells are expected to remain defective for absent *FIG2*-mediated cell wall assembly or organization functions, it may not be surprising that they still possess reduced integrity relative to wild-type cells. Studies by other groups have also failed to observe sorbitol suppression of viability defects induced by mating morphogenesis in the

mid2 and *spc110* mutants (24, 41, 57). Perhaps the continuous polarized growth targeting involved in mating projection morphogenesis presents a potential cell integrity challenge that cannot be rescued in the time frame for mating or of such studies. Other groups have noted a significant level of cell death associated with passage through the mating process in both budding and fission yeasts (8), confirming general observations that this process is inherently dangerous for fungal cells (31, 42, 63).

Adhesins perform diverse cellular roles as pathway target genes. It is interesting that different adhesins, Fig2p, Aga1p, and Sag1/Agα 1p and Flo11p represent the products of terminal differentiation genes of the mating and pseudohyphal/invasive growth pathways, respectively. These genes modulate cell-cell adhesion, and these adhesion differences relative to vegetative cells, along with specific morphogenetic roles of Fig2p, help regulate growth forms. Here we have shown that *FIG2* is required to maintain cell integrity during mating. Interestingly, another adhesin-related gene *SED1*, which encodes a protein predicted to contain two WCPL domains similar to those found in Fig2p and Aga1p (53), has recently been identified as a target of Rho1/Pkc1 pathway activation by genome-wide expression array analysis (22). Taken together, these results suggest that some adhesins such as Fig2p, Flo11p, and perhaps Sed1p may have evolved to assume additional or independent functions, such as cell wall organization, during differentiated phases of the fungal life cycle.

Our studies also further highlight the necessity of the Rho1/Pkc1 pathway and cell wall resident proteins in properly regulating polarized morphogenesis. The activity of this pathway is evidently carefully controlled by feedback loops that appear to help maintain the normal targeting of polarized growth and integrity of cells during mating. The function of Fig2p, the product of a terminal target gene of the mating MAPK signaling pathway influences the extent to which this pathway stimulates activation of the Rho1/Pkc1 cell integrity MAPK pathway during mating. We look forward to the identification and further study of adhesins in other fungi and eukaryotes that may play similarly diverse roles in cellular differentiation and polarized cell growth processes.

ACKNOWLEDGMENTS

We thank S. Vidan and M. Snyder, T. Huffaker, and D. Levin for plasmids and S. Vidan for advice concerning assays of Mpk1 activation. J. Belote and N. Mackin provided comments on the manuscript. We also acknowledge C. Jue and P. Lipke for communication of results prior to publication.

D. Bennett was supported by funds from the Ruth Meyer Scholars fund of Syracuse University.

REFERENCES

1. **Appeltauer, U., and T. Achstetter.** 1989. Hormone-induced expression of the *CHS1* gene from *Saccharomyces cerevisiae*. Eur. J. Biochem. **181:**243–247.
2. **Baudin, A., O. Ozier-Kalogeropoulos, A. Denouel, F. Lacroute, and C. Cullin.** 1993. A simple and efficient method for direct gene deletion in *Saccharomyces cerevisiae*. Nucleic Acids Res. **21:**3329–3330.
3. **Bloom, K.** 2000. It's a kar9ochore to capture microtubules. Nat. Cell Biol. **2:**E96–E98.
4. **Buehrer, B. M., and B. Errede.** 1997. Coordination of the mating and cell integrity mitogen-activated protein kinase pathways in *Saccharomyces cerevisiae*. Mol. Cell. Biol. **17:**6517–6525.
5. **Bulawa, C. E., M. Slater, E. Cabib, J. Au-Young, A. Sburlati, W. J. Adair, and P. W. Robbins.** 1986. The *S. cerevisiae* structural gene for chitin synthase is not required for chitin synthesis *in vivo*. Cell **46:**213–225.
6. **Bussey, H.** 1996. Cell shape determination: a pivotal role for Rho. Science **272:**224–225.
7. **Butty, A. C., P. M. Pryciak, L. S. Huang, I. Herskowitz, and M. Peter.** 1998. The role of Far1p in linking the heterotrimeric G protein to polarity establishment proteins during yeast mating. Science **282:**1511–1516.
8. **Calleja, G. B., B. Y. Yoo, and B. F. Johnson.** 1977. Fusion and erosion of cell walls during conjugation in the fission yeast (*Schizosaccharomyces pombe*). J. Cell Sci. **25:**139–155.
9. **Caro, L. H., H. Tettelin, J. H. Vossen, A. F. Ram, H. van den Ende, and F. M. Klis.** 1997. In silicio identification of glycosyl-phosphatidylinositol-anchored plasma-membrane and cell wall proteins of *Saccharomyces cerevisiae*. Yeast **13:**1477–1489.
10. **Chant, J.** 1999. Cell polarity in yeast. Annu. Rev. Cell Dev. Biol. **15:**365–391.
11. **Chen, D., B. Yang, and T. Kuo.** 1992. One-step transformation of yeast in stationary phase. Curr. Genet. **21:**83–84.
12. **Costigan, C., D. Kolodrubetz, and M. Snyder.** 1994. *NHP6A* and *NHP6B*, which encode HMG1-like proteins, are candidates for downstream components of the yeast *SLT2* mitogen-activated protein kinase pathway. Mol. Cell. Biol. **14:**2391–2403.
13. **Costigan, C., and M. Snyder.** 1994. *SLK 1*, a yeast homolog of MAP kinase activators, has a RAS/cAMP-independent role in nutrient sensing. Mol. Gen. Genet. **243:**286–296.
14. **Delley, P. A., and M. Hall.** 1999. Cell wall stress depolarizes cell growth via hyperactivation of *RHO1*. J. Cell Biol. **147:**163–174.
15. **Erdman, S. E., L. Lin, M. Malczynski, and M. Snyder.** 1998. Pheromone-regulated genes required for yeast mating differentiation. J. Cell Biol. **140:**461–483.
16. **Gammie, A. E., V. Brizzio, and M. D. Rose.** 1998. Distinct morphological phenotypes of cell fusion mutants. Mol. Biol. Cell **9:**1395–1410.
17. **Gulli, M. P., and M. Peter.** 2001. Temporal and spatial regulation of Rho-type guanine-nucleotide exchange factors: the yeast perspective. Genes Dev. **15:**365–379.
18. **Guo, B., C. A. Styles, Q. Feng, and G. R. Fink.** 2000. A *Saccharomyces* gene family involved in invasive growth, cell-cell adhesion, and mating. Proc. Natl. Acad. Sci. USA **97:**12158–12163.
19. **Harrison, J., E. Bardes, Y. Ohya, and D. Lew.** 2001. A role for the Pkc1p/Mpk1p kinase cascade in the morphogenesis checkpoint. Nat. Cell Biol. **3:**417–420.
20. **Hostetter, M. K.** 1994. Adhesins and ligands involved in the interaction of *Candida* spp. with epithelial and endothelial surfaces. Clin. Microbiol. Rev. **7:**29–42.
21. **Iida, H., H. Nakamura, T. Ono, M. Okumura, and Y. Anraku.** 1994. *MID1*, a novel *Saccharomyces cerevisiae* gene encoding a plasma membrane protein, is required for Ca^{2+} influx and mating. Mol. Cell. Biol. **14:**8259–8271.
22. **Jung, U. S., and D. E. Levin.** 1999. Genome-wide analysis of gene expression regulated by the yeast cell wall integrity signalling pathway. Mol. Microbiol. **34:**1049–1057.
23. **Kamada, Y., H. Qadota, C. Python, Y. Anraku, Y. Ohya, and D. Levin.** 1996. Activation of yeast protein kinase C by Rho1 GTPase. J. Biol. Chem. **271:**9193–9196.
24. **Ketela, T., R. Green, and H. Bussey.** 1999. *Saccharomyces cerevisiae* Mid2p is a potential cell wall stress sensor and upstream activator of the *PKC1-MPK1* cell integrity pathway. J. Bacteriol. **181:**3330–3340.
25. **Klis, F. M.** 1994. Cell wall assembly in yeast. Yeast **10:**851–869.
26. **Levin, D. E., and E. Bartlett-Heubusch.** 1992. Mutants in the *S. cerevisiae PKC1* gene display a cell cycle-specific osmotic stability defect. J. Cell Biol. **116:**1221–1229.
27. **Lipke, P. N., and J. Kurjan.** 1992. Sexual agglutination in budding yeasts: structure, function, and regulation of adhesion glycoproteins. Microbiol. Rev. **56:**180–194.
28. **Lipke, P. N., A. Taylor, and C. E. Ballou.** 1976. Morphogenic effects of α-factor on *Saccharomyces cerevisiae* **a** cells. J. Bacteriol. **127:**610–618.
29. **Madden, K., Y. Sheu, K. Baetz, B. Andrews, and M. Snyder.** 1997. SBF cell cycle regulator as a target of the yeast PKC-MAP kinase pathway. Science **275:**1781–1784.
30. **Manning, B. D., R. Padmanabha, and M. Snyder.** 1997. The Rho-GEF Rom2p localizes to sites of polarized cell growth and participates in cytoskeletal functions in *Saccharomyces cerevisiae*. Mol. Biol. Cell **8:**1829–1844.
31. **Marsh, L., and M. D. Rose.** 1997. The pathway of cell and nuclear fusion during mating in *S. cerevisiae*, p. 827–888. *In* J. R. Pringle, J. R. Broach, and E. W. Jones (ed.), The molecular and cellular biology of the yeast *Saccharomyces*, vol. 3. Cold Spring Harbor Laboratory Press, Cold Spring Harbor, N.Y.
32. **Mazur, P., N. Morin, W. Baginsky, M. El-Sherbeini, J. A. Clemas, J. B. Nielsen, and F. Foor.** 1995. Differential expression and function of two homologous subunits of yeast 1,3-β-D-glucan synthase. Mol. Cell. Biol. **15:**5671–5681.
33. **Miller, R., D. Matheos, and M. Rose.** 1999. The cortical localization of the microtubule orientation protein, Kar9p, is dependent upon actin and proteins required for polarization. J. Cell Biol. **144:**963–975.
34. **Miller, R., and M. Rose.** 1998. Kar9p is a novel cortical protein required for cytoplasmic microtubule orientation in yeast. J. Cell Biol. **140:**377–390.

35. **Moser, M., J. Geiser, and T. Davis.** 1996. Ca^{2+}-calmodulin promotes survival of pheromone-induced growth arrest by activation of calcineurin and Ca^{2+}-calmodulin-dependent protein kinase. Mol. Cell. Biol. **16:**4824–4831.
36. **Moskow, J. J., A. S. Gladfelter, R. E. Lamson, P. M. Pryciak, and D. J. Lew.** 2000. Role of Cdc42p in pheromone-stimulated signal transduction in *Saccharomyces cerevisiae*. Mol. Cell. Biol. **20:**7559–7571.
37. **Nern, A., and R. A. Arkowitz.** 1999. A Cdc24p-Far1p-gbetagamma protein complex required for yeast orientation during mating. J. Cell Biol. **144:**1187–1202.
38. **Orlean, P.** 1997. Biogenesis of yeast wall and surface components, p. 229–362. *In* J. R. Pringle, J. R. Broach, and E. W. Jones (ed.), The molecular and cellular biology of the yeast *Saccharomyces*, vol. 3. Cold Spring Harbor Laboratory Press, Cold Spring Harbor, N.Y.
39. **Page, B., and M. Snyder.** 1993. Chromosome segregation in yeast. Annu. Rev. Microbiol. **47:**231–261.
40. **Paravicini, G., M. Cooper, L. Friedli, D. J. Smith, J.-L. Carpentier, L. S. Klig, and M. A. Payton.** 1992. The osmotic integrity of the yeast cell requires a functional *PKC1* gene product. Mol. Cell. Biol. **12:**4896–4905.
41. **Philip, B., and D. E. Levin.** 2001. Wsc1 and Mid2 are cell surface sensors for cell wall integrity signaling that act through Rom2, a guanine nucleotide exchange factor for Rho1. Mol. Cell. Biol. **21:**271–280.
42. **Philips, J., and I. Herskowitz.** 1997. Osmotic balance regulates cell fusion during mating in *Saccharomyces cerevisiae*. J. Cell Biol. **138:**961–974.
43. **Pruyne, D., and A. Bretscher.** 2000. Polarization of cell growth in yeast. I. Establishment and maintenance of polarity states. J. Cell Sci. **113:**365–375.
44. **Qadota, H., I. Ishii, A. Fujiyama, Y. Ohya, and Y. Anraku.** 1992. *RHO* gene products, putative small GTP-binding proteins, are important for activation of the *CAL1*/*CDC43* gene product, a protein geranylgeranyl-transferase in *Saccharomyces cerevisiae*. Yeast **8:**735–741.
45. **Rajavel, M., B. Philip, B. M. Buehrer, B. Errede, and D. E. Levin.** 1999. Mid2 is a putative sensor for cell integrity signaling in *Saccharomyces cerevisiae*. Mol. Cell. Biol. **19:**3969–3976.
46. **Reynolds, T. B., and G. R. Fink.** 2001. Bakers' yeast, a model for fungal biofilm formation. Science **291:**878–881.
47. **Roberts, C., B. Nelson, M. Marton, R. Stoughton, M. Meyer, H. Bennett, Y. He, H. Dai, W. Walker, T. Hughes, M. Tyers, C. Boone, and S. Friend.** 2000. Signaling and circuitry of multiple MAPK pathways revealed by a matrix of global gene expression profiles. Science **287:**873–880.
48. **Roemer, T., G. Paravicini, M. Payton, and H. Bussey.** 1994. Characterization of the yeast (1–6)-β-glucan biosythetic components, Kre6p and Skn1p, and genetic interactions between the *PKC1* pathway and extracellular matrix assembly. J. Cell Biol. **127:**567–579.
49. **Sambrook, J., E. F. Fritsch, and T. Maniatis.** 1989. Molecular cloning: a laboratory manual, 2nd ed. Cold Spring Harbor Laboratory Press, Cold Spring Harbor, N.Y.
50. **Scheckman, R., and V. Brawley.** 1979. Localized deposition of chitin on the yeast cell surface in response to mating pheromone. Proc. Natl. Acad. Sci. USA **76:**645.
51. **Segal, M., and K. Bloom.** 2001. Control of spindle polarity and orientation in *Saccharomyces cerevisiae*. Trends Cell Biol. **11:**160–166.
52. **Segall, J. E.** 1993. Polarization of yeast cells in spatial gradients of α-factor. Proc. Natl. Acad. Sci. USA **90:**8332–8336.
53. **Sharkey, L. L., M. D. McNemar, S. M. Saporito-Irwin, P. S. Sypherd, and W. A. Fonzi.** 1999. *HWP1* functions in the morphological development of *Candida albicans* downstream of *EFG1*, *TUP1*, and *RBF1*. J. Bacteriol. **181:**5273–5279.
54. **Sherman, F., G. R. Fink, and J. Hicks.** 1986. Methods in yeast genetics. Cold Spring Harbor Laboratory Press, Cold Spring Harbor, N.Y.
55. **Smits, G., H. van den Ende, and F. Klis.** 2001. Differential regulation of cell wall biogenesis during growth and development in yeast. Microbiology **147:**781–794.
56. **Sprague, G. F., and J. Thorner.** 1992. Pheromone response and signal transduction during the mating process of *Saccharomyces cerevisiae*, p. 657–744. *In* J. R. Broach, J. R. Pringle, and E. W. Jones (ed.), The molecular biology of the yeast *Saccharomyces*, vol 2. Cold Spring Harbor Laboratory, Cold Spring Harbor, N.Y.
57. **Stirling, D., and M. Stark.** 2000. Mutations in *SPC110*, encoding the yeast spindle pole body calmodulin-binding protein, cause defects in cell integrity as well as spindle formation. Biochim. Biophys. Acta **1499:**85–100.
58. **Sundstrom, P.** 1999. Adhesins in *Candida albicans*. Curr. Opin. Microbiol. **2:**353–357.
59. **Terrance, K., and P. N. Lipke.** 1981. Sexual agglutination in *Saccharomyces cerevisiae*. J. Bacteriol. **148:**889–896.
60. **van der Vaart, J. M., R. Biesebeke, J. W. Chapman, H. Y. Toschka, F. M. Klis, and C. T. Verrips.** 1997. Comparison of cell wall proteins of *Saccharomyces cerevisiae* as anchors for cell surface expression of heterologous proteins. Appl. Environ. Microbiol. **63:**615–620.
61. **Wang, P., and T. Huffaker.** 1997. Stu2p: a microtubule-binding protein that is an essential component of the yeast spindle pole body. J. Cell Biol. **139:**1271–1280.
62. **Wendland, J.** 2001. Comparison of morphogenetic networks of filamentous fungi and yeast. Fungal Genet. Biol. **34:**63–82.
63. **White, J. M., and M. D. Rose.** 2001. Yeast mating: getting close to membrane merger. Curr. Biol. **11:**R16–R20.
64. **Winzeler, E., D. Shoemaker, A. Astromoff, H. Liang, K. Anderson, B. Andre, R. Bangham, R. Benito, J. Boeke, H. Bussey, A. Chu, C. Connelly, K. Davis, F. Dietrich, S. Dow, M. El Bakkoury, F. Foury, S. Friend, E. Gentalen, G. Giaever, J. Hegemann, T. Jones, M. Laub, H. Liao, R. W. Davis et al.** 1999. Functional characterization of the *S. cerevisiae* genome by gene deletion and parallel analysis. Science **285:**901–906.
65. **Zarzov, P., C. Mazzoni, and C. Mann.** 1996. The SLT2(MPK1) MAP kinase is activated during periods of polarized cell growth in yeast. EMBO J. **15:**83–91.